

## A method for direct thalamic stimulation in fMRI studies using a glass-coated carbon fiber electrode

Bai-Chuang Shyu<sup>a,\*</sup>, Chun-Yu Lin<sup>a</sup>, Jyh-Jang Sun<sup>a</sup>,  
Sergiy Sylantyev<sup>b</sup>, Chen Chang<sup>a</sup>

<sup>a</sup> Institute of Biomedical Sciences, Academia Sinica, Taipei 115, Taiwan, ROC

<sup>b</sup> Odesa National Mechnikov University, Odesa 65026, Ukraine

Received 15 December 2003; received in revised form 13 February 2004; accepted 16 February 2004

### Abstract

Recent fMRI studies are of interest in exploring long-range interactions between different brain structures and the functional activation of specific brain regions by known neuroanatomical pathways. One of the experimental approaches requires the invasive implantation of an intracranial electrode to excite specific brain structures. In the present report, we describe a procedure for the production of a glass-coated carbon fiber electrode and the use of this electrode for direct activation of the brain in fMRI studies. The glass-coated carbon fiber microelectrode was implanted in the medial thalamus of anaesthetized rats and T<sub>2</sub>\*-weighted gradient echo images in the sagittal plane obtained on a 4.7 T system (Biospec BMT 47/40) during electrical stimulation of the medial thalamus. The image quality obtained using this electrode was acceptable without reduction of the signal-to-noise ratio and image distortion. Cross-correlation analysis showed that the signal intensities of activated areas in the ipsilateral anterior cingulate cortex were significantly increased by about 4–5% during medial thalamus stimulation. The present study shows that glass-coated carbon fiber electrodes are suitable for fMRI studies and can be used to investigate functional thalamocingulate activation.

© 2004 Elsevier B.V. All rights reserved.

**Keywords:** Carbon fiber electrode; Medial thalamus; Anterior cingulate cortex; Electrical stimulation; MR compatibility

### 1. Introduction

Invasive stimulation of a deep brain region has been used in patients with intractable pain (Duncan et al., 1991; Kumar et al., 1997), Parkinson's disease (Antonini et al., 2003; Patel et al., 2003; Pesenti et al., 2003), and dystonia (Krauss, 2003; Kupsch et al., 2003). Visual targeting of the electrode location using magnetic resonance imaging (MRI) has been shown to be effective in shortening the time required for implantation and, because of its accuracy, in improving the clinical symptoms (Starr et al., 2002; Patel et al., 2003). Several MR-compatible electrical stimulation methods for use in humans have been developed (Dormont et al., 1997; Liem and van Dongen, 1997; Obler et al., 1999; Rezai et al., 2001), but the interference elicited by metal electrodes in a strong magnetic field is still a potential problem in functional

MRI (fMRI) studies, in which susceptibility artifacts may result in image degradation (Berthezene et al., 1997; Obler et al., 1999).

In a recent fMRI study in animals, we showed that stainless steel or tungsten microelectrodes have a strong susceptibility effect and that the BOLD signal drops off significantly around the electrode (Lin et al., 2002; Shyu et al., 2004). An alternative method using carbon fiber electrodes for direct brain stimulation in animal fMRI studies has been reported by ourselves and others (Lin et al., 2002; Austin et al., 2003). Carbon fiber electrodes have been used for electrophysiological studies and for voltammetric analysis of transmitters in vivo, and their use for extracellular recording can result in significantly less noise (Crespi et al., 1995; Dressman et al., 2002). Since carbon fiber has a low conductance, the tip of a carbon fiber microelectrode can pass current efficiently if its impedance can be matched with the output impedance of the current pulse generator. Furthermore, since carbon fiber has very weak paramagnetic properties compared to other conventional electrodes, it is an ideal candidate for use in

\* Corresponding author. Tel.: +886-2-2652-3915;

fax: +886-2-2782-9224.

E-mail address: bmbai@ccvax.sinica.edu.tw (B.-C. Shyu).

deep brain electrical stimulation in fMRI studies in animals, in which the brain area is much smaller than in humans and the susceptibility artifact is more significant.

In our recent electrophysiological studies, we verified the specific transmission pathway from the medial thalamus (MT) to the anterior cingulate cortex (ACC) (Hsu and Shyu, 1997; Hsu et al., 2000; Kung and Shyu, 2002). The MT and ACC are central to the medial pain system subserving the affective and emotional aspects of painful experiences (Vogt and Sikes, 2000) and it was therefore pertinent to test the feasibility of using carbon fiber electrodes for functional activation of this thalamocingulate pathway. In the present report, we describe the production of the glass-coated carbon fiber electrode and fMRI signal changes in the ACC activated by the MT-implanted carbon fiber electrode in anaesthetized animals.

## 2. Materials and methods

### 2.1. Experimental animals

A total of eight male Sprague–Dawley rats (250–350 g body weight) were used and were housed five to a cage in a room with an artificial light system (lights on from 7 a.m. to 7 p.m.) at a temperature of 22 °C with free access to food and water. All experiments were carried out in accordance with the guidelines established by the Academia Sinica Institutional Animal Care and Utilization Committee.

### 2.2. Production of the glass-coated carbon fiber electrode

The glass used in the carbon fiber electrode was single barrel standard borosilicate capillary glass without a micro-filament, with an outer diameter of 1.5 mm and an i.d. of 1.0 mm (A-M Systems Inc., USA). The carbon fiber bundle was obtained from the Formosa Plastics Group (Taiwan, ROC). The manufacture of the glass-coated carbon fiber electrode involved several steps.

- (1) Cutting the micropipette to a length of 15 cm and teasing out a thin thread of carbon fiber from the bundle (Fig. 1a).
- (2) Insertion of the carbon fiber thread into the glass pipette (Fig. 1b).
- (3) Pulling of the pipette containing the carbon fiber using a vertical micropipette puller (Model 730, David Kopf Instruments, USA), resulting in two micropipettes connected by the carbon fibers (Fig. 1c).
- (4) Cutting the carbon fibers and trimming the tip so that the only region at which carbon fiber is exposed about 0.2 mm in the extreme end of the electrode tip (Fig. 1d).
- (5) Bending the pipette into a right-angle on the flame of a benzene lamp (Fig. 1e). The pipette shank was held horizontal at one end and the part beyond the heating point allowed to drop to the vertical when the glass was melted.
- (6) Measurement of the impedance (Fig. 1f).

The end of the thread of carbon fibers extending from the end of the glass-coated carbon fiber electrode was twisted around the end of another thread of carbon fibers inserted in another PE-50 tube. The reference electrode consisted of a thin thread of carbon fibers, about 0.5 mm in thickness, inserted into a PE-50 tube. These two electrodes were placed parallel to each other and the PE-50 tubes fixed together using dental cement (Fig. 1g).

The impedance of the glass-coated carbon fiber electrodes, measured using an electrode impedance tester (model BL-1000-B, Winston Electronics Co., USA) at 135 Hz, was approximately 1 mΩ. To ensure that the coated glass insulation was intact up to the electrode tip, electrodes with impedances lower than 0.5 mΩ were discarded. Since a surface coil, which was used to detect the radio frequency (RF) signals, was attached to the top of the rat's head during fMRI experiments, leaving no space between the coil and the scalp, a right-angle bend was made in the electrode shank approximately 7.0 mm from the electrode tip, allowing it to be implanted completely inside the brain tissue and the scalp to be sutured flat after electrode implantation. The total length of the finished glass electrode was approximately 15 cm.

### 2.3. Surgical preparation of the animals

This part of the experimental procedure was carried out in a laboratory separate from the MRI scanner room. The rats were given atropine (6 mg/kg, i.p.), then anesthetized with pentothal (50 mg/kg, i.p.). A PE-240 tube was inserted by tracheotomy for later artificial ventilation in the scanner, and a PE-50 tube for drug infusion was inserted into the left femoral vein. Following surgery, xylocaine (5%, Astra, Sweden) was applied to the tissue surrounding the wound to reduce nociception and eliminate excitation from peripheral tissue, then the rats were mounted on a stereotaxic apparatus (David Kopf Instruments, USA). The rectal temperature was measured with a thermal couple and maintained at  $36.5 \pm 0.5$  °C using a homeothermo blanket system (Harvard Apparatus, USA).

Craniotomy was performed and a hole made at stereotaxic coordinates 2.5 mm posterior to the bregma and 1.0 mm lateral to the midline, then the dura in the hole was carefully removed using fine scissors. The glass-coated carbon fiber electrode, held by a manipulator, was inserted through the hole into the left MT (5 mm below the cortical surface), while the reference electrode was inserted into the nearby connective tissue beneath the scalp and parallel to the stimulating electrode. Both electrodes were fixed in place on the skull with dental cement, then the scalp was sutured flat to make a good contact with the surface coil in the next step. The carbon fiber-containing PE-50 tubes were com-

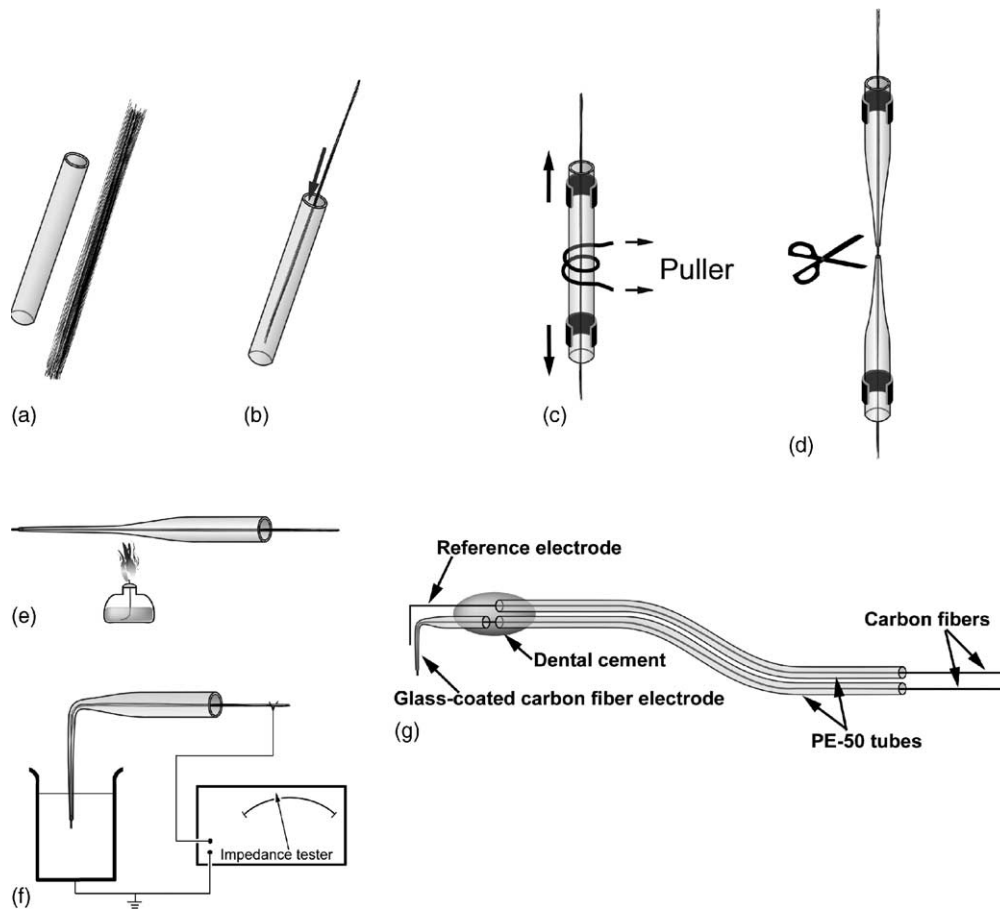


Fig. 1. Procedure for producing the glass-coated carbon fiber electrode. (a) Borosilicate capillary glass and carbon fibers. (b) Insertion of thin carbon fiber thread into the glass pipette. (c) Pulling the carbon fiber-containing pipette. (d) Cutting and trimming of the tip of the glass-coated carbon fiber electrode. (e) Bending of the electrode. (f) Electrode impedance measurement. (g) The glass-coated carbon fiber electrode and reference electrode fixed together.

pletely covered by skin, the carbon fibers surfacing through the neck skin. The set-up for the electrodes is shown in Fig. 2.

#### 2.4. Set-up of the implanted animal in the magnet

The animal was transferred from the laboratory to the MRI scanner room and fixed in place in a custom-made holder. The surface coil was mounted on top of the scalp (Fig. 2), then a muscle relaxant (gallamine triethiodide, 50 mg/kg, i.v.) was administered and artificial ventilation commenced (small animal ventilator, Model 683, Harvard Instrument, USA). The CO<sub>2</sub> concentration of the exhaled breath was monitored constantly on a CO<sub>2</sub> monitor (Normcap 200 oxy, Detax Instrumentarium Corp., Finland) and controlled within the range of 3.5–4.5%. The rectal temperature was measured with an optical fiber probe (Model 790, Luxtron Instrument, USA) and maintained at  $36.5 \pm 0.5^\circ\text{C}$  by a custom-made feedback-controlled warm-air system. A supplementary dose of pentothal (10 mg/kg/h, i.v.) was given after the rat was moved into the magnetic core. Tail pinch-

ing was used periodically to test the depth of anesthesia. If the pinch induced a withdrawal movement or a decrease in end tidal CO<sub>2</sub> concentration, a supplementary dose of anesthetics was given.

The pair of carbon fiber threads protruding from the neck skin was connected via copper plugs to a pair of 2 m long copper wires extending outside the cage insulating the scanner which were connected to the output of a pulse generator (Model 2100, A-M Systems Inc., USA). The cathode end of the output was connected to the wire leading to the carbon fiber electrode. The ventilation equipment, CO<sub>2</sub> monitor, thermometer and stimulator were all situated outside the cage and connected by cables to the animal inside the magnet.

#### 2.5. MRI acquisition system

fMRI experiments were performed on a 4.7 T horizontal bore magnet (Biospec BMT 47/40, Bruker Instruments, Germany) equipped with an actively shielded gradient system (0–5.9 G/cm in 500  $\mu\text{s}$ ). A 20 cm volume coil was

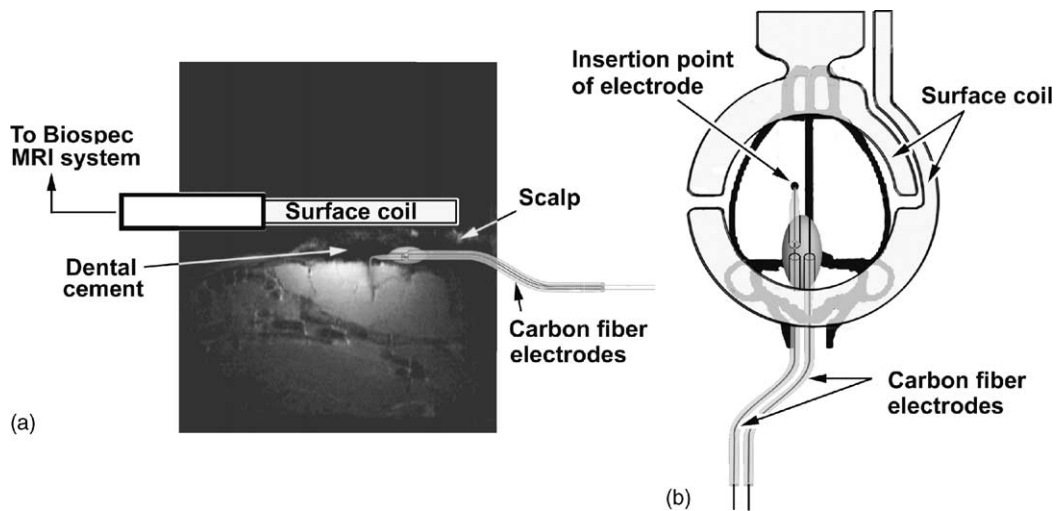


Fig. 2. Arrangement of the glass-coated carbon fiber electrode and surface coil, relative to the brain. (a) A diagram showing the position of the electrodes and surface coil is superimposed on a  $T_2$ -image in the sagittal plane. Electrodes were fixed by dental cement beneath the scalp and the surface coil mounted on top of the scalp. (b) Top view showing the relative positions of the electrodes, surface coil, and brain. Using the image, the insertion point of the electrode is adjusted to be near the center of the surface coil to obtain optimal functional signals from the underlying brain tissue.

used for RF transmission and a 2 cm surface coil for reception.

## 2.6. Positioning the head

$T_1$ -weighted spin-echo (SE) images were scanned in the transverse, coronal, and sagittal planes to correctly position the animal's head so that the brain images were centered at 1 mm posterior to the bregma.

## 2.7. fMRI imaging acquisition

$T_2^*$ -weighted gradient-echo (GE) images in the sagittal plane were collected with a repetition time (TR) of 213.5 ms, an echo time (TE) of 30 ms, a flip angle of  $22.5^\circ$ , a field of view of 5 cm, 4 signal averages, and a slice thickness of 2 mm. The acquisition matrix was  $256 \times 128$  with a matrix of  $256 \times 256$  after zero-filling. The images covered the rat brain from 2 mm left of the midline to the midline and ipsilateral to the stimulating site. The total scanning time for each image was approximately 109 s. To assess brain functional activation by electrical stimulation, an OFF/ON stimulation sequence was employed. A series of 21  $T_2^*$ -weighted GE images in the sagittal plane was collected during the periods of no stimulation (images 1–5, 10–13, and 18–21) and the two periods of electrical stimulation (images 6–9 and 14–17). The first image was a dummy scan and was not analyzed. Four images were taken in each OFF and ON period. Stimulation consisted of rectangular current pulses of  $300 \mu\text{A}$ , 0.2 ms duration, and 10 Hz frequency. The relative timing of each scanning image was illustrated in the time and imaging number scales in Fig. 5d.

## 2.8. Fine anatomical localization using $T_2$ -imaging

To identify the anatomical location of the functional image,  $T_2$ -weighted SE images in the sagittal plane were acquired using a TR of 4 s, a TE of 80 ms, a field of view of 5 cm, 2 averages, and a slice thickness of 2 mm. The acquisition matrix was  $256 \times 128$  with a matrix of  $256 \times 256$  after zero-filling.

## 2.9. Imaging data processing

Image data processing and analyses were performed using MRVision (MRVision Co., USA) running on a Silicon Graphics INDY workstation. The image data were processed as described previously (Chang and Shyu, 2001). Based on the structures in the sagittal plane in the atlas (Paxinos and Watson, 1998; Fig. 5b), a region of interest (ROI) within the ACC or MT was selected on the  $T_2$ -weighted anatomical images. The MRVision program was used to determine the total pixel number within the selected ROI of the ACC and MT from the  $t$ -statistic image and to calculate the mean signal intensity for all of the activated pixels. Functional activation was measured by calculating the percentage change in the averaged signals between baseline (first OFF period, images 2–5) and each of the two ON periods (images 6–9 and 14–17).

## 2.10. Histology

At the end of the fMRI experiment, a small electrolytic lesion ( $20 \mu\text{A}$  for 30 s, anodal DC) was made in the MT at the location of the carbon fiber electrode tip. The rats were anaesthetized with a high dose of sodium pentobarbi-

tal (60 mg/kg, i.p.), then fixed at room temperature by transcardial perfusion with 200 ml of saline followed by 200 ml of 4% paraformaldehyde in 0.1 M sodium phosphate buffer, pH 7.4. The brains were sliced with a freezing microtome into 50  $\mu$ m thick coronal sections which were stained with Cresyl violet.

### 3. Results

#### 3.1. Positioning of the glass-coated-carbon fiber electrode

Three different planes of SE images were used to align the head and assess the correct placement of the electrode. Examples of images in the coronal, horizontal and sagittal planes are shown in Fig. 3(a–c), respectively; the electrode track (shown by the white arrow) can be distinguished from the surrounding brain tissue. In this and three other experiments, the electrode was successfully implanted into the MT.

#### 3.2. $T_2^*$ -GE images in the sagittal plane

Typical examples of sagittal GE images from an animal implanted in the MT with a glass-coated carbon fiber electrode and from a non-implanted animal are shown in Fig. 4a and b, respectively. The carbon fiber electrode caused only minimal interference (the arrow points to the vertical track), which was limited to the region of the electrode. ANOVA results for groups of four animals showed that the signal-to-noise ratios in the ACC and MT of the implanted group did not differ significantly from those in the control group (data not shown).

#### 3.3. Brain regions activated by direct MT stimulation

The activated brain image using a glass-coated carbon fiber electrode implanted in the MT is shown in Fig. 5a and the corresponding anatomical structures from the standard atlas (Paxinos and Watson, 1998) are shown in Fig. 5b. Fig. 5c shows the relative position of the sagittal slice used in Fig. 5a on a top view of a  $T_2$ -image in the horizontal plane.

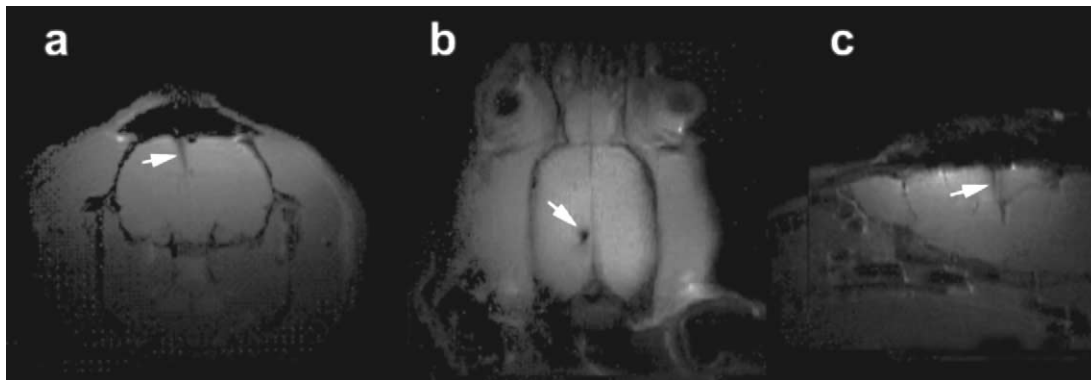


Fig. 3. Coronal (a), horizontal (b), and sagittal (c) planes of  $T_1$ -images of a brain implanted with a glass-coated carbon fiber electrode. The white arrows indicate the electrode track.

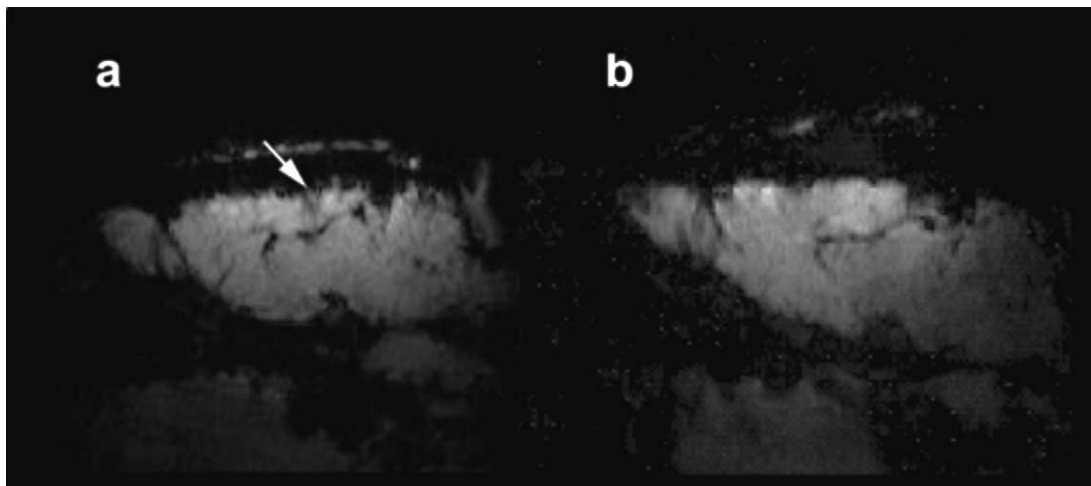


Fig. 4.  $T_2^*$ -GE images in the sagittal plane of a brain with (a) or without (b) implantation of a glass-coated carbon fiber electrode. The white arrow points to the electrode track.

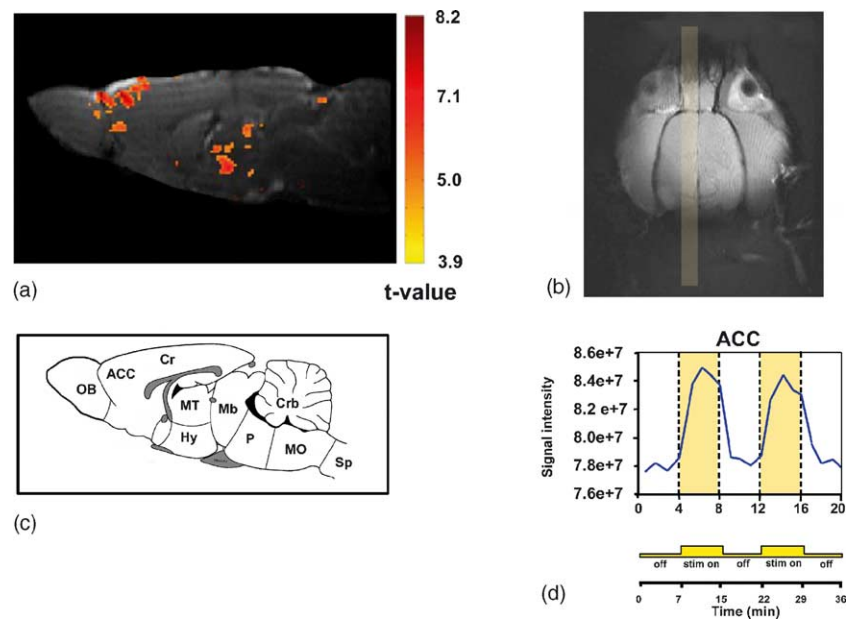


Fig. 5. Functional brain images and activation time-course for the ACC. (a) Functional signals overlaid on a sagittal plane T<sub>2</sub>-image showing areas activated during electrical stimulation using a glass-coated carbon fiber electrode implanted in the MT. Marked activity is seen in the ACC and MT. The color bar indicates the statistic *t*-value. (b) The anatomical structures, taken from the standard Paxinos and Watson atlas, at a level of 0.40 mm lateral to the midline, corresponding to the T<sub>2</sub>-image shown in (a). ACC, anterior cingulate cortex; Cr, cerebral cortex; Crb, cerebellum; Hy, hypothalamus; MO, medulla oblongata; Mb, midbrain; MT, medial thalamus; OB, olfactory bulb; P, pons; SP, spinal cord. (c) The position of the sagittal slice shown on a top view of a T<sub>2</sub>-image. (d) Changes in signal intensity with time in the ACC during two periods of 10 Hz electrical stimulation using a glass-coated carbon fiber electrode (stimulation periods shown by the bar under the panels). The signals are the averaged values over the ROI of the ACC.

Table 1

The total activated pixel number and percent increase of MR signals in the ACC and MT of four experimental rats

Experimental rats	ACC			MT		
	Activated pixel number	First ON period (%)	Second ON period (%)	Activated pixel number	First ON period (%)	Second ON period (%)
fz0508	48.00	3.94	1.04	91.00	7.50	4.99
fz0523	232.00	7.07	7.48	173.00	7.93	6.53
fz0925	198.00	3.98	3.86	169.00	5.23	3.63
fz1029	42.00	4.76	7.92	2.00	4.12	2.89

Marked activation was seen in the ACC region, as well as at the MT stimulation site. Measurement of the change in signal intensity in the ACC with time showed a rapid increase on stimulation and a decrease to baseline levels within a few minutes of stimulus cessation (Fig. 5d). The relative timing of the scanning images was indicated in the time scale. The total activated pixel number and percent increase in the MR signal in four experimental rats are shown in Table 1. An approximately 4–5% increase in signal was seen in both the ACC and MT. In contrast, no activated pixels or signal increase were seen in 4 implanted, but non-stimulated, live control rats.

### 3.4. Stimulation sites of implanted carbon fiber electrodes

An example of the histological verification of a MT stimulation site implanted with a glass-coated carbon fiber electrode is shown in Fig. 6. The lesion mark can be seen as an irregular gray circular area in the ventral part of the lateral

mediodorsal thalamic nucleus (MDL) (Fig. 6b). The histological section was taken 2.56 mm posterior to the bregma. Similar results were obtained in another three experiments.

## 4. Discussion

In this paper, we describe the production of a glass-coated carbon fiber electrode and show that this electrode is MR-compatible and suitable for use in fMRI studies of brain activation. Functional brain activation in the thalamocingulate pathway was detected using this deep brain electrical stimulation method in anaesthetized animals.

### 4.1. Electrode fabrication

In our previous study (Lin et al., 2002), we demonstrated that the glass-coated carbon fiber electrode was superior to metal-containing electrodes, such as tungsten and stainless

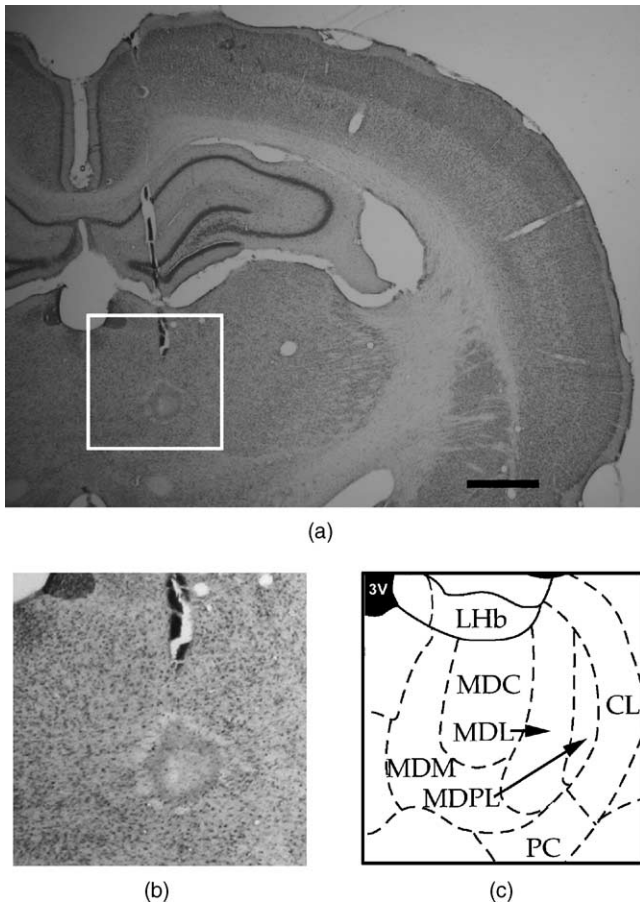


Fig. 6. Histological verification of the stimulation site. (a) Transverse section of a brain implanted with a glass-coated carbon fiber electrode. The electrode track and the lesion mark at the bottom of the track can be seen. The region including the lesion mark covered by the white square is shown enlarged in (b) and (c). The corresponding anatomical structures taken from the atlas,  $-2.56$  mm posterior to the bregma. CL, centrolateral thalamic nucleus; D3V, dorsal third ventricle; Lhb, lateral habenular nucleus; MDC, central mediodorsal thalamic nucleus; MDM, medial mediodorsal thalamic nucleus; MDL, lateral mediodorsal thalamic nucleus; MDPL, paralaminar mediodorsal thalamic nucleus; PC, paracentral thalamic nucleus. Scale bar = 1 mm in (a) and 0.5 mm in (b).

steel electrodes, since the high susceptibility caused by these readily available metal electrodes results not only in signal loss, but also in image distortion, and makes it difficult to evaluate the functional images obtained following excitation of the pathway. The glass-coated carbon fiber electrode was manufactured entirely manually. Initially, the entire procedure took approximately one hour and the success rate was about 50%, but, with practice, the time required was reduced to less than 45 min and the successful rate increased to 80%.

#### 4.2. Insulation and impedance

To ensure that the electrical current is delivered only to the electrode tip so that a specific brain structure can be excited, good insulation is a crucial factor. The glass coat of the shank of the electrode is very fragile. When trimming

the carbon fiber at the electrode tip using scissors, the glass around the tip can sometimes be damaged, so care has to be taken at this stage, as a greater tip area results in a lower current density being delivered through the tip. Good insulation of the carbon fiber electrode can be judged by a high impedance, and we have found that an electrode with an impedance of  $1\text{ m}\Omega$  is acceptable for implantation.

#### 4.3. Correct placement of the stimulating electrode

Based on existing knowledge of neuroanatomical pathways, a projected brain area would be expected to be activated following stimulation of the appropriate brain area, and fMRI signal changes would be expected in the projected area if the origin is precisely targeted for stimulation. Thus, the correct placement of the stimulating electrode is another critical factor. The resolution of  $T_1$ - and  $T_2$ -images is not high enough to distinguish the position of the electrode tip and, using a tungsten electrode, it has been shown that, if the stimulating electrode in the MT is moved vertically by only 0.5 mm, the evoked extracellular field potentials in the ACC are lost (Kung and Shyu, 2002). In pilot experiments, we checked the electrophysiological responses in the ACC using a tungsten recording microelectrode before fixing the electrodes to the skull with dental cement, and found that the quality of the electrophysiological responses obtained prior to electrode fixation was a good indicator of the quality of the fMRI signals after electrode fixation, suggesting that electrophysiological verification could be routinely performed to assess the correct placement of the electrode.

#### 4.4. Fixing of the electrode to the skull

Dental cement was used to fix the electrode in place. However, since the skull is flat and fixation can be problem if no anchoring point is attached. One factor causing detachment of the dental cement is the infiltration of fluid or blood into the space between the cement and the skull, so it is important to dry the skull and cauterize the bleeding site on the skull surface by electrocautery before applying the dental cement. A ceramic screw fixed to the skull can provide an additional anchoring point for dental cement fixation.

#### 4.5. Electrode interference

The recent use of deep brain electrical stimulation in human fMRI studies shows that it should be possible to perform safe functional MR imaging by modifying not only the tip region of the electrode, but also the arrangement of the electrodes, connecting wires, and coil (Gleason et al., 1992; Berthezene et al., 1997; Obler et al., 1999; Tronnier et al., 1999; Alwatban et al., 2002; Rezai et al., 2002). One of the concerns about MR compatibility is the interaction between the electrode and the time-varying magnetic field in the presence of a conducting loop (Tenforde, 1986). In our experimental set-up, the induced current was minimized by

decreasing the area of the conducting loop, and the conducting loop was arranged approximately parallel to the B1 field and so should induce a lower voltage within the RF field. In addition, the impedance of the carbon fiber electrode was approximately 1 M $\Omega$ , higher than those for conventional electrodes, making it possible to reduce the induced electrical current (Obler et al., 1999).

#### 4.6. Alternative approach

In the present acute study, the animals were paralyzed and artificial ventilation maintained during the experiment. This approach was used to immobilize the animal, resulting in good quality images. Chronic implantation can also be performed, using the same animal preparation method as for acute experiments except for the insertion of the tracheal tube and venous catheter. In this case, the animal will breathe spontaneously and not be paralyzed. Supplementary anesthetics should be supplied by intraperitoneal injection. To obtain long-term and more durable fixation of the implanted electrodes, we recommend using a ceramic screw fixed to the skull to provide additional anchoring. Since the artifact and shift caused by spontaneous head or body movement is unavoidable, a misregistration correction should be included in the image analysis.

In conclusion, the present method is useful for exploring temporal and spatial BOLD signal changes in different brain areas which can be evoked using a nonparamagnetic carbon fiber electrode implanted in a deep brain structure to excite a known specific neuroanatomical pathway. The electrode and animal can be prepared for acute and chronic implantation and, in the latter case, changes in functional brain activation can be studied over a long period using fMRI.

#### Acknowledgements

We thank Mr. Tsung-Hung Hung for assistance with the art work and Dr. Thomas Barkas for English revision. This study was supported by grants from the National Science Council and the Academia Sinica, Taiwan, ROC.

#### References

Alwatban AZ, Ludman CN, Mason SM, O'Donoghue GM, Peters AM, Morris PG. A method for the direct electrical stimulation of the auditory system in deaf subjects: a functional magnetic resonance imaging study. *J Magn Reson Imag* 2002;16:6–12.

Antonini A, Marotta G, Benti R, Landi A, De Notaris R, Mariani C, Gerundini P, Pezzoli G, Gaini SM. Brain flow changes before and after deep brain stimulation of the subthalamic nucleus in Parkinson's disease. *Neurol Sci* 2003;24:151–2.

Austin VC, Blamire AM, Grieve SM, O'Neill MJ, Styles P, Matthews PM, Sibson NR. Differences in the BOLD fMRI response to direct and indirect cortical stimulation in the rat. *Magn Reson Med* 2003;49:838–47.

Berthezene Y, Truy E, Morgon A, Giard MH, Hermier M, Franconi JM, Froment JC. Auditory cortex activation in deaf subjects during cochlear electrical stimulation. Evaluation by functional magnetic resonance imaging. *Invest Radiol* 1997;32:297–301.

Chang C, Shyu BC. A fMRI study of brain activations during non-noxious and noxious electrical stimulation of the sciatic nerve of rats. *Brain Res* 2001;897:71–81.

Crespi F, England T, Ratti E, Trist DG. Carbon fibre micro-electrodes for concomitant in vivo electrophysiological and voltammetric measurements: no reciprocal influences. *Neurosci Lett* 1995;188:33–6.

Dormont D, Cornu P, Pidoux B, Bonnet AM, Biondi A, Oppenheim C, Hasboun D, Damier P, Cuchet E, Philippon J, Agid Y, Marsault C. Chronic thalamic stimulation with three-dimensional MR stereotactic guidance. *Am J Neuroradiol* 1997;18:1093–107.

Dressman SF, Peters JL, Michael AC. Carbon fiber microelectrodes with multiple sensing elements for in vivo voltammetry. *J Neurosci Methods* 2002;119:75–81.

Duncan GH, Bushnell MC, Marchand S. Deep brain stimulation: a review of basic research and clinical studies. *Pain* 1991;45:49–59.

Gleason CA, Kaula NF, Hricak H, Schmidt RA, Tanagho EA. The effect of magnetic resonance imagers on implanted neurostimulators. *Pacing Clin Electrophysiol* 1992;15:81–94.

Hsu MM, Shyu BC. Electrophysiological study of the connection between medial thalamus and anterior cingulate cortex in the rat. *Neuroreport* 1997;8:2701–7.

Hsu MM, Kung JC, Shyu BC. Evoked responses of the anterior cingulate cortex to stimulation of the medial thalamus. *Chin J Physiol* 2000;43:81–9.

Krauss JK. Deep brain stimulation for cervical dystonia. *J Neurol Neurosurg Psychiatry* 2003;74:1598.

Kumar K, Toth C, Nath RK. Deep brain stimulation for intractable pain: a 15-year experience. *Neurosurgery* 1997;40:736–46.

Kung JC, Shyu BC. Potentiation of local field potentials in the anterior cingulate cortex evoked by the stimulation of the medial thalamic nuclei in rats. *Brain Res* 2002;953:37–44.

Kupsch A, Klaffke S, Kuhn AA, Meissner W, Arnold G, Schneider GH, Maier-Hauff K, Trottenberg T. The effects of frequency in pallidal deep brain stimulation for primary dystonia. *J Neurol* 2003;250:1201–5.

Liem LA, van Dongen VC. Magnetic resonance imaging and spinal cord stimulation systems. *Pain* 1997;70:95–7.

Lin J, Sun S, Chen C, Chang W, Hou B, Shyu BC. A fMRI study of the anterior cingulate cortex activations during direct electrical stimulation of the medial thalamus in rats. In: Proceedings of the 10th World Congress on Pain (Abstract); 2002. p. 48.

Obler R, Kostler H, Weber BP, Mack KF, Becker H. Safe electrical stimulation of the cochlear nerve at the promontory during functional magnetic resonance imaging. *Magn Reson Med* 1999;42:371–8.

Patel NK, Plaha P, O'Sullivan K, McCarter R, Heywood P, Gill SS. MRI directed bilateral stimulation of the subthalamic nucleus in patients with Parkinson's disease. *J Neurol Neurosurg Psychiatry* 2003;74:1631–7.

Paxinos G, Watson C. The rat brain stereotaxic coordinates. 4th ed. San Diego: Academic Press; 1998.

Pesenti A, Priori A, Locatelli M, Egidi M, Rampini P, Tamma F, Caputo E, Chiesa V, Barbieri S. Subthalamic somatosensory evoked potentials in Parkinson's disease. *Mov Disord* 2003;18:1341–5.

Rezaei AR, Finelli D, Rugieri P, Tkach J, Nyenhuis JA, Shellock FG. Neurostimulators: potential for excessive heating of deep brain stimulation electrodes during magnetic resonance imaging. *J Magn Reson Imag* 2001;14:488–9.

Rezaei AR, Finelli D, Nyenhuis JA, Hrdlicka G, Tkach J, Sharan A, Rugieri P, Stypulkowski PH, Shellock FG. Neurostimulation systems for deep brain stimulation: in vitro evaluation of magnetic resonance imaging-related heating at 1.5 tesla. *J Magn Reson Imag* 2002;15:241–50.

Shyu B-C, Lin C-Y, Sun J-J, Chen S-L, Chang C. BOLD response to direct thalamic stimulation reveals functional connection of the medial

- thalamus and anterior cingulate cortex in the rat. *Magn Reson Med* 2004, in press.
- Starr PA, Christine CW, Theodosopoulos PV, Lindsey N, Byrd D, Mosley A, Marks Jr WJ. Implantation of deep brain stimulators into the subthalamic nucleus: technical approach and magnetic resonance imaging-verified lead locations. *J Neurosurg* 2002;97:370–87.
- Tenforde TS. Mechanisms for biological effects of magnetic fields. In: Thomas SR, Dixon RL, editors. *NMR in medicine: instrumentation and clinical applications*. Medical Monograph No. 14. American Association of Physics in Medicine: New York; 1986. pp. 71–92.
- Tronnier VM, Staubert A, Hahnel S, Sarem-Aslani A. Magnetic resonance imaging with implanted neurostimulators: an in vitro and in vivo study. *Neurosurgery* 1999;44:118–25.
- Vogt BA, Sikes RW. The medial pain system, cingulate cortex, and parallel processing of nociceptive information. *Prog Brain Res* 2000;122:223–35.